MAUSAM, **76**, 3 (July 2025), 766-777

MAUSAM

DOI : https://doi.org/10.54302/mausam.v76i3.6684
Homepage: https://mausamjournal.imd.gov.in/index.php/MAUSAM

UDC No. 550.34 (540.11)

Source characterisation of June 2023 Doda (Kashmir) earthquake

SINDU KUMARI[1#], AMBIKAPATHY AMMANI[1*], DELNA JOY K.[1@], VISHWARANJAN OJHA[1$], SANDEEP ARORA[2]

[1]*National Center for Seismology, Ministry of Earth Sciences, New Delhi, India*

([#]sindukumari219@gmail.com, [@]del.kachappilly@gmail.com, [$]vrojha017@gmail.com)

[2]*Banaras Hindu University, Varanasi, Uttar Pradesh, India* (**sandeeparora95@gmail.com)**

(*Received 1 June 2024, Accepted 16 April 2025*)

***Corresponding author's email: ammani.ambikapathy@imd.gov.in**

सार – 13 जून 2023 को 13:33:42 IST पर, जम्मू और कश्मीर (J&K) के डोडा क्षेत्र में Ml5.1 तीव्रता का भूकंप आया। भूकंप का केंद्र 33.15 डिग्री उत्तर और 75.89 डिग्री पूर्व के निर्देशांक पर था, जिसकी उथली गहराई 10 किमी थी। यह भूकंपीय घटना हिमालय की भूगर्भीय पृष्ठभूमि के भीतर हुई, जिसने भारतीय प्लेट और यूरेशियन प्लेट के बीच टकराव के परिणामस्वरूप आकार लिया है। हिमालयी क्षेत्र, इन टेक्टोनिक टकरावों की जटिल गतिशीलता की विशेषता रखता है, जिसमें कई महत्वपूर्ण क्षेत्रीय और स्थानीय दोष प्रणालियाँ हैं। इन दोष रेखाओं का एक बड़ा हिस्सा सक्रिय रहता है, जो लगातार हिमालयी क्षेत्र और उसके आस-पास के क्षेत्रों में भूकंपीय गतिविधि उत्पन्न करता है। स्रोत क्षेत्र में कुछ इमारतों को मामूली संरचनात्मक क्षति पहुँचाने के बावजूद, इस विशेष भूकंप को अच्छी तरह से प्रलेखित किया गया था और भारतीय राष्ट्रीय भूकंपीय नेटवर्क द्वारा सटीक रूप से स्थित किया गया था, जिसे राष्ट्रीय भूकंप विज्ञान केंद्र (NCS), पृथ्वी विज्ञान मंत्रालय (MoES) द्वारा संचालित किया जाता है। उल्लेखनीय रूप से, NCS-MoES जम्मू और कश्मीर (विशेष रूप से जम्मू, श्रीनगर और उधमपुर में) में तीन भूकंपीय वेधशालाओं का रखरखाव करता है, साथ ही लद्दाख में दो अतिरिक्त भूकंपीय वेधशालाएँ (हैनली और अलची में) भी हैं। वर्तमान अध्ययन में, हमने NCS-MoES द्वारा प्रबंधित 15 भूकंपीय वेधशालाओं के नेटवर्क से एकत्रित तरंग डेटा का उपयोग किया है, जो रणनीतिक रूप से J&K, लद्दाख और हिमाचल प्रदेश में स्थित हैं। हमारा शोध भूकंप के भौगोलिक स्थान के सटीक निर्धारण सहित स्रोत विशेषताओं का अनुमान लगाने का प्रयास करता है। हमारे विश्लेषण में विशेष सॉफ़्टवेयर टूल, भूकंप के केंद्र के स्थानीयकरण के लिए SEISAN और दोष तल समाधान के लिए ISOLA का उपयोग किया गया। इसके अलावा, इन व्युत्पन्न भूकंपीय मापदंडों ने आगे के विश्लेषणों के लिए आधारभूत डेटा के रूप में कार्य किया। विशेष रूप से, हमने इन मापदंडों का लाभ उठाकर जारी की गई ऊर्जा की मात्रा निर्धारित की और स्रोत त्रिज्या निर्धारित की। इन अतिरिक्त जानकारियों ने इस भूकंप और इसके निहितार्थों की एक व्यापक विशेषता प्रदान की।

ABSTRACT. On the 13th of June 2023, at 13:33:42 IST, an earthquake of magnitude Ml5.1 occurred in the Doda region of Jammu & Kashmir (J&K). The earthquake's epicenter was at coordinates 33.15° N and 75.89° E, with a shallow depth of 10 km. This seismic event unfolded within the geological context of the Himalayan orogeny, which has taken shape as a consequence of the collision between the Indian plate and the Eurasian plate. The Himalayan region, characterized by the intricate dynamics of these tectonic collisions, harbours numerous significant regional and local fault systems. A substantial portion of these fault lines remains active, continually generating seismic activity throughout the Himalayan region and its adjacent areas. Despite causing minor structural damage to a few buildings in the source region, this particular earthquake was well-documented and was accurately located by the Indian National Seismic Network, which is operated by the National Centre for Seismology (NCS), Ministry of Earth Sciences (MoES). Notably, the NCS-MoES maintains three Seismological observatories in Jammu & Kashmir (specifically in Jammu, Srinagar, and Udhampur), along with two additional Seismological observatories in Ladakh (in Hanley and Alchi). In the present study, we have harnessed waveform data collected from a network of 15 Seismological observatories managed by NCS-MoES, strategically positioned across J&K, Ladakh, and Himachal Pradesh. Our research endeavours to estimate the source characteristics including the precise determination of the earthquake's geographical location. Our analysis employed specialized software tools, SEISAN for epicenter localization and ISOLA for fault plane solution. Moreover, these derived seismic parameters served as foundational data for further analyses. Specifically, we leveraged these parameters to quantify the energy released and determine the source radius. These additional insights provided a comprehensive characterization of this earthquake and its implications.

Key words – Doda Region, Eurasian Plate, SEISAN, Source Characteristics, Source Radius.

1. Introduction

The state of Jammu and Kashmir, situated in the north-western part of India, occupies a highly tectonically active region within the expansive Himalayan arc. It shares borders with China to the east, Pakistan to the west, Afghanistan to the north, and the plains of Punjab and Himachal Pradesh to the south and south-east, respectively. Geographically, it spans from 32° 17' to 37° 05' latitude North and 72° 31' to 80° 20' longitude East, encompassing a length of around 640 km from north to south and a width of over 480 km from east to west. The state is characterized by three distinct regions: the Kashmir Valley, Jammu, and Ladakh. Jammu and Kashmir have a historic seismic activity, with past earthquakes leaving their mark on the region. Notably, the 2005 Kashmir earthquake, with a magnitude of 7.6, stands out as one of the deadliest earthquakes in human history. It resulted in the tragic loss of over 100 thousand lives and widespread destruction of critical infrastructure. This seismic event brought the region vulnerability to earthquakes into sharp focus. Subsequent population growth and the development of unscientific and unplanned infrastructure have heightened the risk of damage from recurring earthquakes in the region. The study area, specifically the Doda region, is situated near the rupture zones of significant historical earthquakes, including the 2005 Muzaffarabad earthquake (Mw 7.6) (Jan *et al.*, 2008), the 1885 Sopore earthquake (Mw 6.0) (Banghar *et al.*, 1972; Ambraseys and Douglas., 2004), and the 2013 Jangalwar earthquake (Mw 5.7) (Pandey *et al.*, 2017). This entire region has experienced intense geological forces, including faulting and folding, due to the ongoing Himalayan orogeny. These geological processes are intrinsically linked to the seismic activity observed in the area. In the field of seismology, parameters characterizing the source of an earthquake are referred to as earthquake source parameters. These critical parameters are derived from measurements of seismic phase arrival times in the time domain and the spectral characteristics of seismic waves in the frequency domain pioneers for this Richter, introduced a magnitude parameter to accurately quantify the size of an earthquake based on the amplitude of its seismic waveform. Brune, 1970 further advancement by developing a scaling law that enable the calculation of source parameters using seismic wave spectra. These parameters play a pivotal role in determining various aspects of an earthquake source, including seismic moment, source radius and stress drop, etc. The information gained from analysed earthquake characteristics plays a key role in many seismology and engineering studies. This data helps us understand how earthquakes work, predict their effects, and improve the design of buildings and infrastructure to with stand future events.

Seismotectonic & geology of the region

The Kashmir Valley occupies a prominent position, it is one of the most seismically active regions of the Himalayan arc, rendering it susceptible to earthquakes originating from both nearby and distant sources. Over its geological history, the region has witness numerous significant earthquakes, ranging from intensity levels VIII to X. These seismic events have inflicted substantial damage to both human-made and natural structures in the area. Geologically, the Union territory of Jammu and Kashmir comes under Seismic Zones V and IV. Its formation is intricately linked to the continental-continental collision between the Indian and Eurasian plates, culminating in the development of the Kashmir piggy back basin in the latter stages of this ongoing tectonic convergence (Burbank and Johnson, 1983). Over time, a substantial 1300-meter-thick layer of deposits, ranging from Plio-Pleistocene to Holocene, has accumulated in the basin. These deposits comprise glacio-fluvial-aeolian-lacustrine unconsolidated sediments. The active movement along the NE dipping Kashmir Basin Fault (KBF) has significantly influenced the geomorphology of the basin. The Kashmir Valley exhibits a rich geological diversity, featuring all three major rock types, namely sedimentary, metamorphic, and igneous rocks. These rocks span from the Precambrian Salkhala to more recent formations. Moving to the Doda region, which is situated between the Panjal Thrust (PT) and the Chenab Normal Thrust (CNF). The entire Doda-Kishtwar region (DKR) lies amidst extensional and compressional structures (Searle, 1989; Stephenson *et al.*, 2021). This region occupies a central position in the north-western Himalaya, near the Chenab Normal Fault. It is characterized by a Proterozoic basement overlain by the extensively deformed and polymetamorphic High Himalayan Crystalline (HHC) Complex, which comprises schist, gneiss, migmatite and intrusions of granitoid and leucogranite. Notably, along the Main Central Thrust (MCT), the high-grade HHC rocks thrust over the lower to medium-grade metasedimentary series of the Lesser Himalaya. The Lesser Himalayan Sequence in this region is confined between the Main Boundary Thrust and the Main Central Thrust, forming a narrow zone. Additionally, the Lesser Himalayan rocks emerge as the Kishtwar Window, encompassed and overlain by the medium-range metamorphic HHC (Fig. 1). These Lesser Himalayan rocks are seen as thrust sheets in the region (Bhanot *et al.*, 1975). Notably, along the Main Central Thrust (MCT), the high-grade HHC rocks thrust over the lower to medium-grade meta sedimentary series of the Lesser Himalaya. The Lesser Himalayan sequence in this region is confined between the Main Boundary Thrust and the Main Central Thrust, forming a narrow zone. Additionally, the Lesser

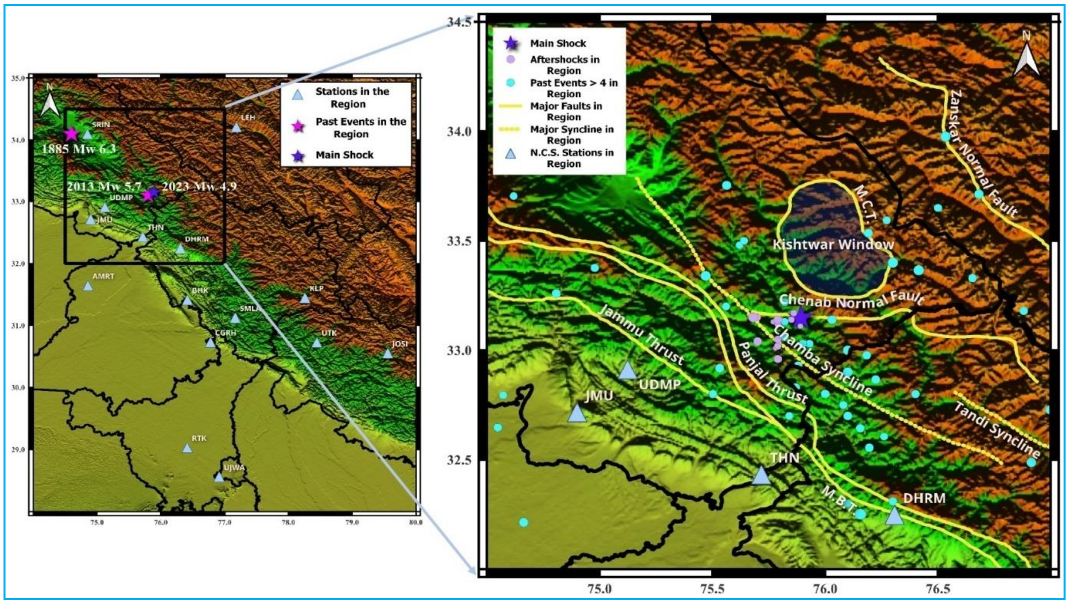

Fig. 1. Topographic map of the Doda and surrounding region superimposed with major tectonic features as well as regional seismicity modified after Horton *et al.* (2015), Dasgupta *et al.* (2000). Labels signify as MBT (Main Boundary Thrust), MCT (Main Central Thrust), Doda (13 June, 2023, 13:33:42 IST, M 5.1) earthquakes are shown in blue star and big red colour beach ball is the Fault plane solution of the main event

Himalayan rocks emerge as the Kishtwar Window, encompassed and overlain by the medium-range metamorphic HHC (Fig. 1). The Doda region and its surroundings are marked by significant geological features, including major faults such as the Main Boundary Thrust, Panjal Thrust, Main Central Thrust, Kishtwar Fault (KF), and Chenab Normal Fault. Syncline structures like the Chamba syncline and Tandi syncline are also prominent in the area. In the southern part, the crystalline rocks of the Higher Himalayan Zone thrust over the Main Central Thrust (MCT), extending from the Kishtwar Window to the Thatri area near Jangalwar (Jangpangi, 1986). Here, the Bhaderwah Formation, comprising quartzite, quartzitic slate, and slate, overlays the rocks of the Thatri region, locally referred to as the Chenab Higher Himalayan Crystalline (Thakur *et al.*, 1995). Throughout the Kishtwar region, extensive faulting and folding have played a vitalrole in shaping the geological landscape, coinciding with the broader Himalayan mountain-building processes (Singh, 2010; Haq *et al.*, 2019). The region features younger gneissose and schistose rocks overlain by Older Quartzites along the Kishtwar Thrust, while the younger volcanic and sedimentary rocks are found along the Chamba Thrust, encompassing the granitic and metamorphic rocks of the Kishtwar Group (Wakhaloo and Shah, 1970; Wakhaloo and Dhar, 1971). This geological complexity underscores the dynamic and intricate history of the Kashmir Valley and the Doda region, revealing the diverse rock formations and structural forces that have shaped these landscapes over millennia.

2. Data collection and analysis

In pursuit of a comprehensive understanding of the source characteristics of the June 2023 earthquake in Doda, Kashmir, we conducted an in-depth analysis. In this study we have used data collected from 15 permanent seismic 3-component Broadband Seismograph (BBS) stations, all part of the network established by the NCS-MoES.

These seismic stations are situated in close proximity to the major regional faults within the regions of Jammu & Kashmir, Ladakh, Himachal Pradesh, Uttarakhand, Haryana, and New Delhi (Table 1). Each of these seismic stations is equipped with advanced equipment, including Trillium 240, Trillium 120QA, and Reftek 151B-120 sensors, along with a Centaur data collection system. The seismic data are continuously recorded at a sampling rate of 40 samples per second. The seismic data obtained from all 15 stations played a crucial role in determining critical parameters such as the earthquake's epicenter location and the source characteristics of both the main event and its subsequent aftershocks.

Seismograms derived from these recordings are rich sources of information, encapsulating insights into the

TABLE 1

Stations location and Epicentral distance

S. No.	Name of the Station (State)	Station Code	Latitude (°N)	Longitude (°E)	Epicentral Distance (km)
1.	Udhampur (J&K)	UDMP	32.913	75.124	76
2.	Thein Dam (Punjab)	THN	32.433	75.717	81
3.	Jammu (J&K)	JMU	32.717	74.9	104
4.	Dharamshala (H.P)	DHRM	32.248	76.307	107
5.	Srinagar (J&K)	SRIN	34.1	74.85	143
6.	Alchi (Leh)	ALCI	34.214	77.184	168
7.	Rohtak (Haryana)	RTK	29.033	76.414	188
8.	Amritsar (Punjab)	AMRT	31.6459	74.857	193
9.	Bhakra (H.P)	BHK	31.417	76.417	199
10.	Shimla (H.P)	SMLA	31.128	77.167	255
11.	Chandigarh	CGRH	30.733	76.779	281
12.	Kalpa (H.P)	KLP	31.45	78.26	285
13.	Uttarkashi (Uttarakhand)	UTK	30.73	78.446	361
14.	Joshimath (Uttarakhand)	JOSI	30.556	79.558	450
15.	Najafgarh (Delhi)	UJWA	28.562	76.915	519

TABLE 2

Location of June 2023, Doda, Kashmir earthquake and its aftershocks

S. No.	Origin time (UTC)		Latitude (°N)	Longitude (°E)	Depth (Km)	Magnitude (Ml)
	YYYY/MM/DD	HR:MM:SEC				
1.	2023/06/13	08:03:42	33.15	75.89	10	5.1
2.	2023/06/13	20:50:57	33.15	75.84	09	4.2
3.	2023/06/13	21:11:40	33.17	75.81	10	2.5
4.	2023/06/14	02:26:46	33.22	75.86	20	3.1
5.	2023/06/14	02:59:34	33.14	75.85	5	3.3
6.	2023/06/14	10:30:03	33.17	75.86	5	3.3
7.	2023/06/17	16:25:35	33.22	75.78	10	4.3
8.	2023/06/17	22:20:26	33.22	75.91	10	4.0
9.	2023/06/17	23:52:09	33.01	75.78	10	2.7
10.	2023/07/10	00:08:54	33.15	75.68	10	4.9
11.	2023/07/10	00:13:44	33.15	75.70	8	3.6
12.	2023/07/17	16:37:26	33.05	75.79	5	3.8
13.	2023/08/07	18:34:48	33.02	75.79	5	3.7
14.	2023/08/18	11:43:03	33.21	76.09	5	3
15.	2023/09/01	10:18:03	33.11	75.89	4	2.9

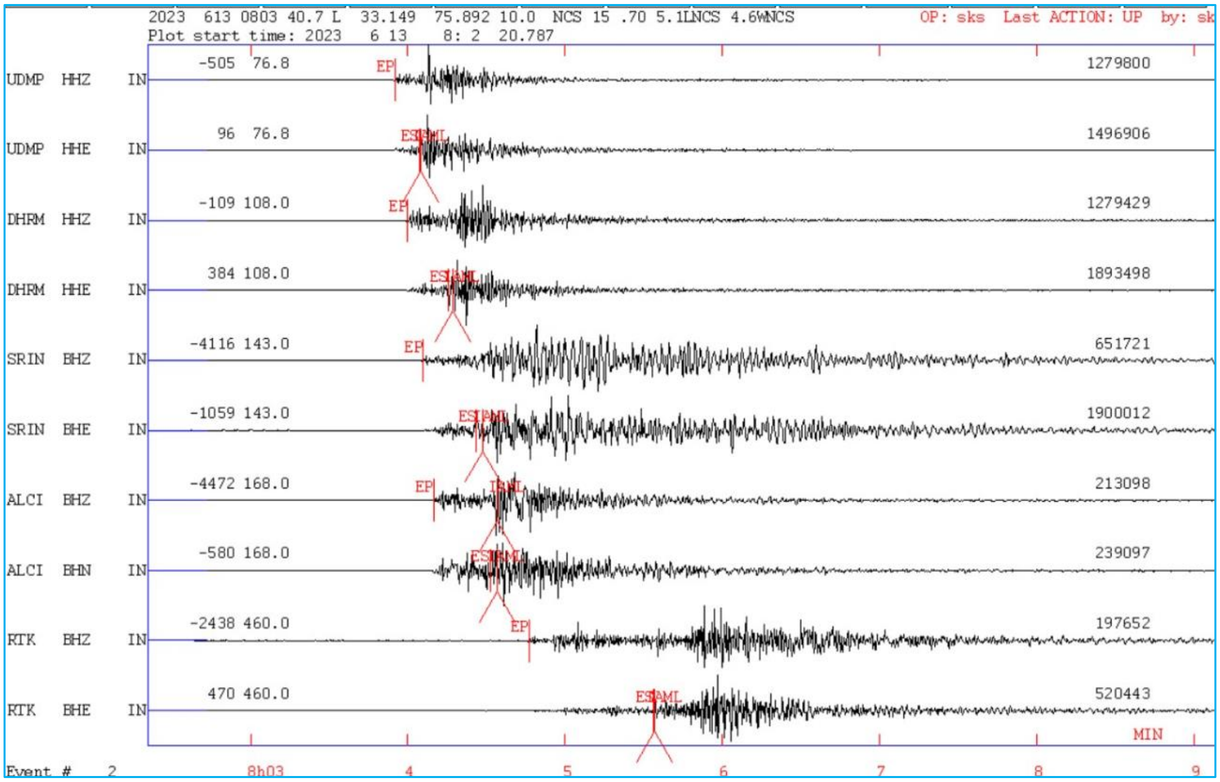

Fig. 2. Waveforms records for the 13th June, 2023 Doda earthquake by nearest BBS network installed by NCS-MoES. The body phases (P-S waves) are marked in red colour (EP for P-waves and ES for S-waves)

earthquake's source, the characteristics of the geological site and the propagation path of seismic waves. Consequently, they are invaluable for estimating the effects related to the earthquake's source, site, and propagation. To process and analyse this seismic data, we use the SEISAN software package, as developed by (Havskov and Ottemoller in 1999). This software facilitated the relocation of seismic events and the estimation of critical source parameters, ultimately contributing to a more comprehensive understanding of the earthquake and its associated dynamics.

2.1. *Earthquake location*

The earthquake that struck Doda on June 13, 2023, at 1:33 PM IST, was carefully recorded by 15 Broadband Seismic (BBS) stations within a 500 km range. These stations are part of the NCS-MoES network, which actively monitors earthquakes. Almost fifteen earthquakes followed this event recorded by NCS-MoES network within two months tabulated in Table 2. This comprehensive coverage provided a robust azimuthal view of the seismic event, as depicted in Fig. 1. The essential details of the seismic stations that played a key role in locating the epicentre and estimating source parameters for both the primary earthquake and its subsequent aftershocks are meticulously outlined in Table 1. This table also includes the respective epicentral distances from the primary shock, offering critical spatial context for the analysis. To facilitate the relocation of these seismic events, a 1-D velocity model established by Kumar *et al.*, 2009 specifically designed for the Kangra-Chambal Himalaya region, was employed. This velocity model includes five different layers located at depths of 0.0, 10.0, 15.0, 18.0 and 46.0 km. Each layer has its own unique P-wave speed, with values of 5.27, 5.55, 5.45, 6.24 and 8.25 km/s, respectively.

The SEISAN software package, a powerful tool for seismological analysis, was employed in conjunction with this velocity model. This software aided in estimating the coordinates of the relocated event, pinpointing them at 33.149° N and 75.892° E, with a notable root mean square (rms) error of merely 0.45 seconds. Additionally, the focal depth of the earthquake was determined to be 10 km, further enhancing the precision of the analysis.

The meticulous work involved in this analysis, is further illustrated in Fig. 2, which showcases the carefully marked phases and amplitudes at each of the five nearest

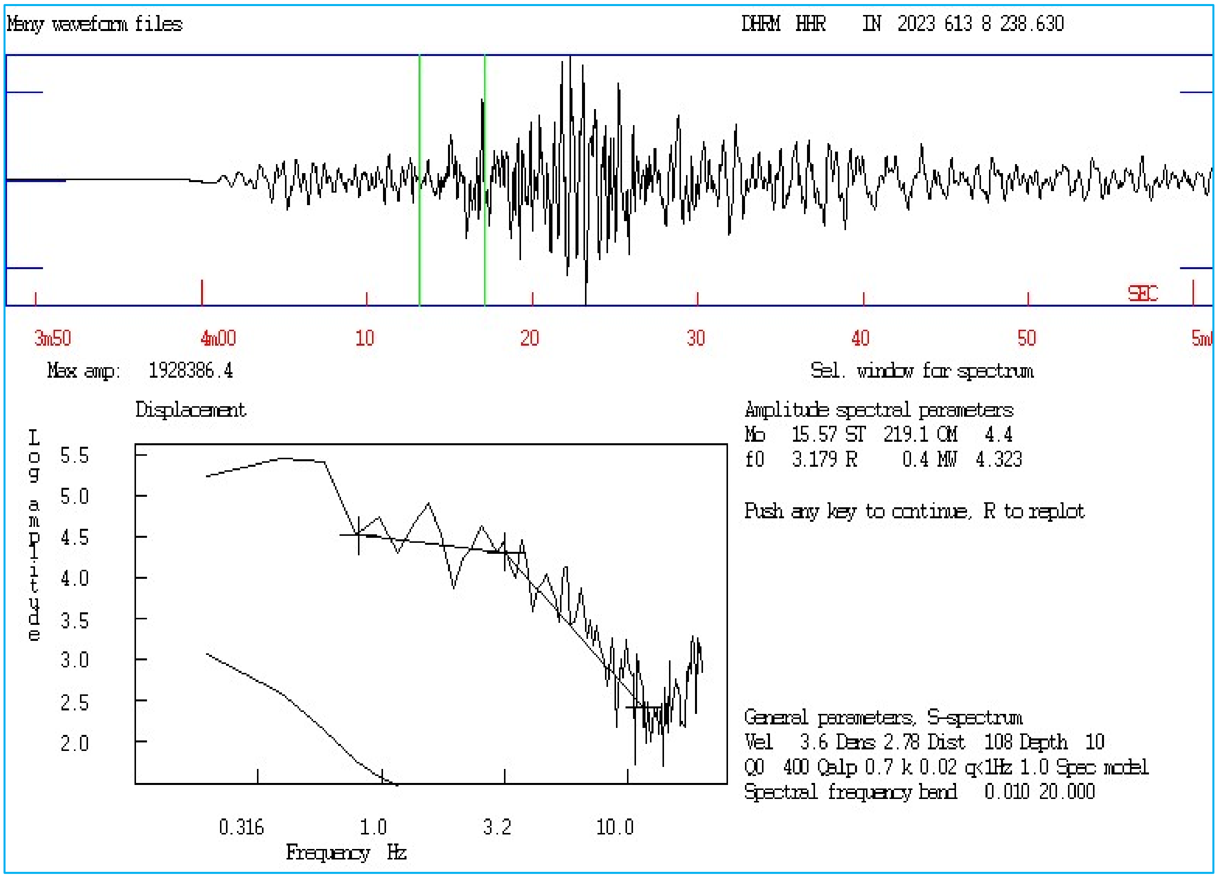

Fig. 3. Displacement amplitude spectra of rotated vertical component of the 13 June, 2023 event (Mw 4.8) recorded by the nearby station located at Dharamsala (DHRM) for the estimation of source parameters

seismic stations, providing a visual representation of the analysis process. The accuracy of the location in latitude and longitude was estimated to be about ± 0.1 km and ± 0.3 km respectively; however, the focal depth is accurate to 10 km. Local magnitude (Ml) 5.1 was estimated by using 15 permanent BBS stations.

2.2. *Source parameters estimation*

This study used a large and detailed dataset of seismic waves from the earthquake on June 13, 2023. The seismic activity was carefully recorded by 15 well-placed stations across the north-western part of India. To ascertain the vital source parameters of this seismic event, a spectral analysis was undertaken, meticulously processing the acquired waveforms. This analysis was conducted with the assistance of the SEISAN software, a sophisticated tool widely employed in seismological research. The source model utilized for this purpose was Brune's source model, a seminal framework introduced by Brune in 1970, it has since been foundational in seismic analysis.

$$D(f) = \frac{G(r,h) * D(f) * Mo * F * 4 * \pi * \rho * v_{pors}^{3}}{\left[1 + \left(\frac{f}{fc}\right)^{2}\right]} \tag{1}$$

where G (r, h) is geometrical spreading, r is epicentral distance, h is hypo-central depth, D (f) is the diminution function due to anelastic attenuation, f is the frequency, ρ is the density, $v_{p\ or\ s}$ is the velocity of the p or s wave at the source, f_c is the corner frequency and F is a factor of 2.0*0.6 to correct for the free surface effect and radiation pattern.

The diminution function D (f) in eqn. (1) is written as:

$$D(f) = P(f) * \exp\left(\frac{-\pi * f * trtime}{q0 * s * q\alpha}\right) \tag{2}$$

TABLE 3

Source parameters of the main events recorded on the vertical and radial components of the seismometer by the NCS-MoES stations on June,13 2023

Station Code	Component	Omega	F_c	M_o	Stressdrop (bars)	Radius (km)	Moment magnitude (Mw)
ALCI	BHZ	3.4	1.29	15.5	2.3	1.84	4.3
ALCI	BHR	4.9	0.56	16.2	4.7	2.41	4.7
AMRT	HHR	5	0.76	17.2	21	3.12	5.4
AMRT	HHZ	5.5	0.54	17.6	22	4.43	5.2
BHK	BHZ	5	0.57	17.2	9.1	4.2	5.4
BHK	BHR	3.8	1.95	14	1.2	0.69	3.3
DHRM	HHZ	3.5	1.47	15.4	2.7	1.62	4.2
DHRM	HHR	4.4	3.17	16.4	43	1.42	4.9
JMU	BHR	4.4	0.8	16.3	3.3	2.98	4.8
JMU	BHR	3.9	1.4	15.1	6.1	0.96	4
JOSI	BHZ	2.9	0.67	15.4	0.3	3.57	4.2
JOSI	BHR	4.4	0.58	15.9	2.9	2.31	4.6
KLP	BHZ	3.2	0.91	15.6	0.9	2.62	4.3
KLP	BHR	4.6	0.83	16	11	1.62	4.6
RTK	BHZ	2.5	2.15	15	18	0.29	4
RTK	BHR	4.1	1.27	15.6	32	0.32	4.4
SMLA	HHZ	3.5	0.957	15.84	2	2.5	4.5
SMLA	HHR	4.4	1.23	15.8	22	1.1	4.5
SRIN	BHZ	3	1.6	15	1.4	1.49	4
SRIN	BHR	4.6	1.63	15.8	49	0.83	4.5
THN	BHZ	2.4	3.11	14.2	1.7	0.77	3.4
THN	BHR	4.9	1.31	16	39	1.03	4.6
UJWA	BHZ	3	1.29	15.6	2.8	1.84	4.3
UJWA	BHR	4	2.44	15.5	92	0.55	4.3
UTK	BHR	3.5	2.79	13.7	1.9	0.48	3.1

where $tr\ time$ is the travel time from the origin time to the start of the spectral window, q_0 and $q_\propto$ accounts for the spectral amplitude correction and

$$P(f) = \exp(-\pi * K * f) \tag{3}$$

is meant to account for near surface losses (Singh *et al.*, 1979) with the constant kappa (K) having a value of the order 0.04 sec. Anelastic attenuation Q is assumed to be frequency dependent following the relation $Q = q_0 * f^{q_\propto}$. This approach allowed us to determine the source characteristics of the Kashmir Doda earthquake such as corner frequency (f_c), scalar seismic moment (M_0), source radius (r), stress drop ($\Delta\sigma$) and Moment Magnitude (M_w).

The various source parameters are estimated using the below mentioned relationships:

$$M_0 = \frac{4 * \pi * R * \rho * v^3 * \Omega_0}{S_a * R_{\theta\phi}} \tag{4}$$

where Ω_0 is the low-frequency spectral level, S_a is the free state effect and $R_{\theta\phi}$ represents the average radiation pattern and R is the hypo-central distance.

TABLE 4

Displays data for four local seismic events, of magnitude ≥ 4 and their estimated source parameters (seismic moment, moment magnitude, corner frequency, source radius, and stress drop)

Date	Time (UTC) (HH:MM:SS)	Corner Frequency	Seismic Moment (N-m)	Moment Magnitude (Mw)	Source Radius (km)	Stressdrop (MPa)
13/06/2023	08:03:40	1.63	1.96E+16	4.82	0.817	15.70
13/06/2023	20:50:57	5.27	1.47E+15	4.04	0.286	2.75
17/06/2023	16:25:35	5.29	2.11E+15	4.18	0.404	1.39
17/06/2023	22:20:26	2.88	8.38E+14	3.96	0.508	2.79

The source radius (r) and stress drop (Δσ) were estimated following Brune's circular model (Brune., 1970 & 1971) as :

$$r = \frac{0.37 * v_{pors}}{fc} \tag{5}$$

$$\Delta\sigma = \frac{7}{16} * \frac{M_0}{R^3} \tag{6}$$

$$Mw = \frac{2}{3} * \log_{10} M_0 - 10.7 \tag{7}$$

Our analysis, we exclusively employed data acquired from Broadband seismographs, which record ground motion velocity at their installation points. To ensure the accuracy of our results, we meticulously addressed instrument-related effects through a comprehensive deconvolution process. This process accounted for various instrument-related parameters, including the poles and zeros of the instrument and other system-specific details, to effectively remove the instrument response from the recorded waveform. Subsequently, we engaged in a crucial step by rotating the instrument-corrected horizontal components of the seismic wave at each station. Fig. 3, shows displacement amplitude spectra of rotated vertical component of the 13 June, 2023 event (Mw 4.8) recorded by the nearby BBS station located at Dharamsala (DHRM) for the estimation of source parameters. Source parameters of the main events recorded on the vertical and radial components of the other BBS installed by NCS-MoES on 13 June, 2023 is tabulated under Table 3 and Table 4.

These horizontal components, representing the north-south and east-west directions, were well transformed into radial and transverse components, a technique well-documented in the works of (Ram *et al.*, 2005 and Kayal *et al.*, 2009). Following this transformation, the SH (Shear-Horizontal) components at each station were further processed in the frequency domain, ultimately yielding displacement spectra. To account for path effects in the displacement spectra, we applied an attenuation correction to the data. This correction was executed using the formula $\mathrm{Q} = 112 * f^{0.97}$, as provided by (Parvez *et al.*, 2012), in conjunction with the kappa (K) value of 0.40, as suggested by (Chopra *et al.*, 2012). To extract critical seismic parameters, we meticulously analyse the displacement spectra. Two vital parameters were deduced from this analysis. Corner Frequency (f_c) which represents the intersection point of the low and high frequency asymptotes within the displacement spectra and Ω_0 which denotes the low-frequency spectral level, and plays a vital role in determining the source parameters, as indicated in the equations outlined earlier. It's important to note that these calculations involved certain constants that were integral to our analysis. v_s (represents the shear wave velocity in the source region) = 3.6 km/sec; ρ(density) = 2.70 g/cm^3;$R_{\theta\phi}$=0.63 and Sa = 2. These constants were drawn from the works of (Bhat *et al.*, 2013 and Pandey *et al.*, 2017) further ensuring the accuracy and reliability of our seismic analysis.

2.3. *Fault plane solution estimation*

To understand the seismic source of an earthquake, the method of seismic waveform inversion helps in determination of the fault orientation and its characteristics. In this method the synthetic waveforms are generated digitally on the basis of local crustal model and earthquake source parameters. To obtain the fault plane solution of the current event waveform inversion was performed with the help of ISOLA software (Sokos and Zahradnik, 2008); it is based on multiple point sources which uses iterative deconvolution method of Kikuchi and Kanamori (1991). Firstly, the seismic data was converted from MSEED to SAC format through the Seisan software

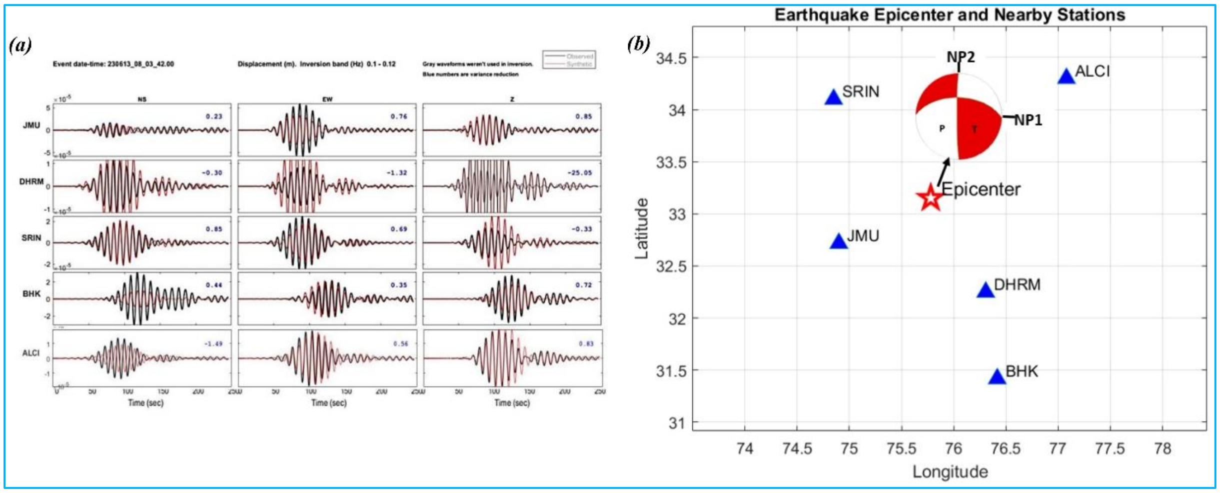

Figs. 4(a&b). (a) Correlation plot for the Mw 4.8 earthquake, observed seismograms are shown as black lines, while synthetic waveforms are depicted in red at five stations. (b) Locations of stations and earthquake used for the matching

TABLE 5

Fault plane solution of the main event

Date &Time (UTC)	Nodal Plane I			Nodal Plane II			Maximum correlation	DC %
	Strike	Dip	Rake	Strike	Dip	Rake		
13/06/2023 (08:03:40)	272°	54°	4°	180°	87°	144°	0.75	77.11

as SAC format is required as an input data to calculate the moment tensor inversion. To compute the full waveform synthetics (Green's functions) discrete wave number method was used by setting a set of pre-defined point source on a plane or a line given by Bouchon, (1981). After getting a major point source contribution, the equivalent synthetics are subtracted from the data. Then, inversion for the remaining waveform for another point source was done, and so on. Consecutively, the point sources are removed one after another, thus each step involves only source position and onset time (Mandal *et al.*, 2017). These two parameters provide stability of the inversion (Zahradnik *et al.*, 2005). After that spatial grid search method is applied to acquire the best source position (location and depth) and time in the form of absolute value of correlation coefficient between the observed and synthetics which are automatically calculated during least square inversion (Zahradnik *et al.*, 2005). The matching between the observed and synthetics after the best fitting of spatio-temporal positions is characterized by the overall variance reduction in all the components of all the stations (Zahradnik *et al.*, 2005). The four band pass filter was applied both to real and synthetic waveforms. The signal to noise ratio curves helps mainly to define first filter, because the noise level limits the usable low-frequency range (Sokos and Zahradnik, 2013). The solution is finalized after getting good correlation between the observed and synthetics waveform along with the high Double Couple (DC %). We used station dependent frequency range according to the signal to noise ratio and the epicentre distance. The deviatoric moment tensor inversion in the ISOLA software was used. For source inversion, the data was processed by applying low-pass filter between the observed and synthetic seismograms along with high DC% the solution was finalized. The different correlation values obtained for the different stations may be due to the different velocity structure depending upon the topography and lithology of the area where stations are located.

First Nodal Plane with strike 272° indicates that the fault plane is oriented roughly west-southwest, which is a horizontal line indicating the direction along which the fault extends. The specific angle suggests that it may be related to regional tectonic features, such as the orientation of nearby plate boundaries or fracture zones. A dip of 54° means the fault plane is inclined significantly.

This steep dip implies that the fault is not shallow and likely affects deeper geological layers. It suggests a potential for significant displacement, particularly in a tectonically active region. Further rake of 4° indicates that the motion along this fault has a very small upward vertical component (toward the hanging wall). This suggests that while there is some vertical movement, it is predominantly a strike-slip mechanism, where lateral movement is the primary characteristic. The low rake suggests minimal thrusting, indicating the fault might behave similarly to a lateral shear fault, but with a slight upward component.

This suggests a left-lateral strike-slip fault with a minor thrust component. The minor upward component suggests that the region is under some tension, which can lead to fractures or slip along the fault. The fault may accommodate lateral motion while also permitting some vertical movement due to compressive stresses. Given its orientation and mechanism, this fault could contribute to surface rupture during seismic events, potentially affecting infrastructure aligned with the fault line.

Considering the second Nodal Plane having strike 180° orientation indicates a fault that runs north-south. The north-south orientation of this fault places it in a direct line with many continental collision zones, suggesting it could be influenced by regional tectonic forces. The nearly vertical dip 87° indicates that this fault is very steep and likely to be a dominant feature in the rock strata. This steepness implies that the fault could be an important conduit for fluids and may influence regional geothermal gradients or earthquake dynamics and a rake of 144° indicates a significant upward movement (toward the hanging wall) and is characteristic of reverse or thrust faults. This suggests that during slip, the hanging wall has moved up relative to the footwall, which is a key characteristic of compressional environments.

This strongly indicative of a reverse (thrust) fault, which is consistent with compressional forces acting on the crust. This fault's steep angle and high rake suggest it is responding to significant compressional stresses, common in regions of continental collision or subduction. It may also indicate uplift of mountain ranges or localized crustal shortening. The steepness and orientation imply that this fault could generate substantial seismic events, potentially affecting a wide area. The mechanics of reverse faults can lead to significant ground shaking, making it a critical focus for hazard assessment.

Considering both the nodal planes located in proximity, they may represent different aspects of a complex tectonic system. NP1's lateral motion may accommodate horizontal strain, while NP2's vertical movement reflects the compressional forces at play. Their interactions could lead to multi-fault systems, where slip on one fault influences the behaviour of the other, raising the likelihood of simultaneous rupture during seismic events. Understanding the broader tectonic framework (*e.g.*, plate boundaries, regional stress fields) is essential to fully interpret these focal mechanisms. The nature of nearby geological features, past seismicity, and local geological history would provide critical context to assess their significance. This detailed interpretation not only aids in understanding the specific mechanisms at play but also informs potential earthquake risks and the geological history of the region.

3. Result and discussion

The epicentre of these seismic events is accurately marked on the geological and seismotectonic map of the Doda region. These events are mainly located between the latitudes of 33.01° to 33.22° N and longitudes of 75.89° to 76.09° E. Their location falls within the geological framework encompassing the Chenab Normal Fault, Panjal Thrust, and Chenab Syncline, as visually depicted in Fig. 1. Upon closer examination of these events, a distinctive feature emerges their shallow depths, which typically range from 4 to 20 km, as detailed in Table 2. The clustering of these shallow-focus earthquakes suggests the potential presence of a detachment zone located above the decollement depth within the Northwestern Himalayan region. Notably, the Northwestern Himalayan region is characterized by the presence of approximately 10 km of sedimentary deposits. Our research findings further unveil a distribution of hypocentres primarily around the southwestern section of the Kishtwar Window, in close proximity to the Chenab Normal Fault. These hypocentres are typically situated at depths ranging from 4 to 20 km. Moreover, a concentration of seismic events, including both the primary 2013 seismic events and their aftershocks, is observable within the region lying between the southwestern segment of the Kishtwar Window and the Panjal Thrust, a pattern clearly illustrated in Fig. 1. For a comprehensive understanding of these seismic events, please refer to Table 4, which presents the estimated source parameters for the four earthquakes of M_w 4 and above that occurred in June 2023, Doda region within close proximity to the main event. These parameters shed further light on the characteristics of these seismic events.

The estimated seismic moment spans a range from 8×10^{21} to 2×10^{23} dyne-cm, while the moment magnitudes of these events vary between 3.9 and 4.8. Additionally, the corner frequencies fall within the range of 1.63 Hz to 5.29 Hz, and the calculated source radii for these events range from 0.28 to 0.81 km. The stress drop of these events exhibits a wide variation, ranging from 13.9 to 157 bars. These findings closely align with results from previous studies conducted in the Himalayan region (Verma *et al.*, 2015). The focal mechanism of the Mw 4.82 earthquake shows a strike slip movement with two nodal planes. One plane strike at 272° with a dip of 54° and rake of 4°, while the other strike at 180° with a dip of 87° and rake of 144°. The northward movement of the Indian Plate towards the Eurasian Plate causes compression in a northeast (NE) direction (Bilham and Wallace, 2005). This collision between the two plates drives the tectonic activity in the region, leading to NE compression on the Indian Plate.

4. Conclusions

By carrying out spectral analysis of body waves obtained from 15 broadband seismographs strategically positioned across the Northwestern Himalayas and its vicinity, this study successfully estimated the source parameters of moderate-sized earthquakes within this region. In line with previous research in active seismic zones, the current study also observed shifts in corner frequencies. The static stress drop value, a critical parameter in seismic analysis, was determined for the earthquakes investigated in this study. These values were found to be distributed within a range of 1.39 to 15.70 MPa, particularly within the week following the occurrence of aftershocks in the region. This observation points to the presence of a significant seismic hazard in the Doda region of the Northwestern Himalayas. Notably, the amplitude of high-frequency ground motions in earthquakes is heavily influenced by stress drop. It is worth emphasizing that stress drop values, spanning the range of 8.38×10^{14} to 1.96×10^{16} N-m, remain consistent regardless of the seismic moment, an intriguing aspect of seismic behavior in this region. The nodal plane orientation suggests a left lateral strike slip fault that links to the Chenab Normal Fault or a nearby offshoot. The recent earthquakes in the Doda area of Chenab Valley might be due to either the reactivation of a fault or the formation of a new thrust branch from the Chenab Normal Fault or Panjal Thrust.

Acknowledgement

The authors express their heartfelt gratitude to Dr. O. P. Mishra, Director of NCS-MoES, for his invaluable support and for providing us with the necessary facilities that were instrumental in the successful completion of this research. Special recognition is also due to Dr. A. P. Singh; Mrs. Poonam Chauhan and Mrs. Gyan Jyoti a key contributor at NCS-MoES, for their timely provision of essential data, which was instrumental in ensuring the timely execution of our research.

Authors' Contributions

Sindu Kumari: Conceptualization.
Ambikapathy Ammani: Supervision, interpretation of results, and reviewed and edited the manuscript.
Delna Joy K: Assisted in waveform analysis, data visualization and validation and interpretation of the results.
Sandeep Arora: literature review and refinement. Vishwaranjan Ojha: assisting in the organization and formatting of references.

Disclaimer: The contents and views presented in this research article/paper are the views of the authors and do not necessarily reflect the views of the organizations they belong to.

References

Ambraseys, N. N. and Douglas, J., 2004, "Magnitude calibration of north Indian earthquakes", *Geophysical Journal International*, **159**, 165-206.

Banghar, A. R., 1972, "Focal mechanisms of Indian earthquakes", *Bulletin of the Seismological Society of America*, **62**, 603-608.

Bhanot, V. B., Goel, A. K., Singh, V. P. and Kwatra, S. K., 1975, "Rb-Sr radiometric studies for the Dalhousie and Rohtang areas, Himachal Pradesh", *Curr. Sci*.(India), **44**, 219-220.

Bhat, G. M., Pandita, S. K., Singh, Yudhbir and Sharma, Sandeep, 2013, "Estimation of source parameters of local earthquakes in Jammu and Kashmir, India", *International Journal of Scientific and Research publications*, **3**.

Bilham, R. and Wallace, K., 2005, "Future Mw> 8 earthquakes in the Himalaya: implications from the 26 Dec 2004 Mw= 9.0 earthquake on India's eastern plate margin", *Geol. Surv. India Spec. Publ*, **85**, 1-14.

Bouchon, M., 1981, "A simple method to calculate Green's functions for elastic layered media", *Bulletin of the Seismological Society of America*, **71**, 4, 959-971.

Brune, James N., 1970, "Tectonic stress and the spectra of seismic shear waves from earthquakes", *Journal of geophysical research*, **75**, 4997-5009.

Burbank, Douglas W. and Gary D., Johnson, 1983, "The late Cenozoic chronologic and stratigraphic development of the Kashmir intermontane basin, northwestern Himalaya", *Palaeogeography, Palaeoclimatology, Palaeoecology*, **43**, 205-235.

Chopra, S., Kumar, V., Suthar, A., & Kumar, P. (2012). Modeling of strong ground motions for 1991 Uttarkashi, 1999 Chamoli earthquakes, and a hypothetical great earthquake in Garhwal–Kumaun Himalaya. *Natural Hazards*, **64,** 2, 1141-1159.

Dasgupta, S., P. Pande, D. Ganguly, Z. Iqbal, K. Sanyal, N. V. Venkataraman, B. Sural *et al.*, 2000, "Seismotectonic Atlas of India and its environments", *Calcutta : Special Publication Geological Survey of India*, **86**.

Havskov, Jens and Lars Ottemoller, 1999, "SEISAN earthquake analysis software", *Seismol. Res. Lett.*, **70**, 532-534.

Horton, F., Lee, J., Hacker, B., Bowman-Kamaha'o, M., & Cosca, M. (2015). Himalayan gneiss dome formation in the middle crust and exhumation by normal faulting: *New geochronology of Gianbul dome, northwestern India. Bulletin*, 127(1-2), 162-180.

Jan, M. Q., Lisa, M. and Khan, M. A., 2008, "Post-October 08, 2005, Muzaffarabad earthquake scenario", *Journal of Himalayan Earth Sciences*, **41**, 2305-6959.

Jangpangi, B. S., Kumar, G., Rathode, D. R. and Dutta, S., 1986, "Geology of the autochthonous folded belt Jammu and Kashmir Himalaya with special reference to Panjal thrust", *Journal of Paleontological Society of India*, **31**, 39-51.

Kayal, J. R., Srivastava, V. K., Bhattacharya, S. N., Khan, P. K. and Chatterjee, R., 2009, "Source parameters and focal mechanisms of local earthquakes : single broadband observatory at ISM, Dhanbad", *Journal of Geological Society of India*, **74**, 413-419.

Kikuchi, M. and Kanamori, H., 1991, "Inversion of complex body waves-III", *Bulletin of the Seismological Society of America*, **81**, 6, 2335-2350.

Kumar, Naresh, Jyoti Sharma, B. R. Arora and Sagarika Mukhopadhyay, 2009, "Seismotectonic model of the Kangra-Chamba sector of Northwest Himalaya : constraints from joint hypocenter determination and focal mechanism", *Bulletin of the Seismological Society of America*, **99**, 95-109.

Mandal, P., Singh, B., Nagendra, P. and Gupta, A. K., 2017, "Modeling of source parameters of the 15 December, 2015 Deogarh earthquake of M w 4.0", *Journal of the Geological Society of India*, **89**, 363-368.

Pandey, S. J., Bhat, G. M., Puri, S., Raina, N., Singh, Y., Pandita, S. K., ... & Sutar, A., 2017, "Seismotectonic study of Kishtwar region of Jammu Province using local broadband seismic data", *Journal of Seismology*, **21**, 525-538.

Parvez, I. A., Yadav, P., & Nagaraj, K. (2012). Attenuation of P, S and coda waves in the NW-Himalayas, India. *International Journal of Geosciences*, **3,** 1, 179-191.

Ram, V. Sri, Kumar, Dinesh and Khattri, K. N., 2005, "The 1986 Dharamsala earthquake of Himachal Himalaya-estimates of source parameters, average intrinsic attenuation and site amplification functions", *Journal of seismology*, **9**, 473-485.

Searle, Michael P. and Rex, A. J., 1989, "Thermal model for the Zanskar Himalaya", *Journal of Metamorphic Geology*, **7**, 127-134.

Singh, Keser, 2010, "Tectonic evolution of Kishtwar window with respect to the Main Central Thrust, northwest Himalaya, India", *Journal of Asian Earth Sciences*, **39**, 125-135.

Sokos, Efthimios N. and Jiri Zahradnik, 2008, "ISOLA a Fortran code and a Matlab GUI to perform multiple-point source inversion of seismic data", *Computers & Geosciences*, **34**, 967-977.

Sokos, E., & Zahradník, J. (2013). Evaluating centroid-moment-tensor uncertainty in the new version of ISOLA software. *Seismological Research Letters*, 84(4), 656-665.

Stephenson, B. J., Searle, M. P., Waters, D. J. and Rex, D. C., 2021, "Structure of the Main Central Thrust zone and extrusion of the High Himalayan deep crustal wedge, Kishtwar-Zanskar Himalaya", *Journal of the Geological Society*, **158**, 637-652.

Thakur, V. C., Rautela, P. and Jafaruddin, M., 1995, "Normal faults in Panjal Thrust Zone n Lesser Himalaya and between the higher Himalaya crystallines and Chamba sequence in Kashmir Himalaya, India", *Proceeding of the Indian Academy of Science -Earth and Planetary science*, **104**, 499-508.

Haq, Ul Ahsan, S. K. Pandita, Yudhbir Singh, G. M. Bhat, Shiv Jyoti Pandey, Arjun Singh, Mithila Verma and Bansal, B. K., 2019, "Evidence of Active Tectonic Deformation in Kishtwar Area, Jammu and Kashmir, Northwest Himalaya, India", *Journal of the Geological Society of India*, **93**, 331-342.

Verma, Mithila, Anup K. Sutar, Brijesh K. Bansal, B. R. Arora and Bhat, G. M., 2015, "MW 4.9 earthquake of 21 August, 2014 in Kangra region, Northwest Himalaya. Seismotectonics implications", *Journal of Asian Earth Sciences*, **109**, 29-37.

Wakhaloo, S. N. and Dhar, B. L., 1971, "On the geology of the area in and around Kishtwar, Doda district, Kashmir Himalaya", *Himal Geo.*, **1**, 123-146.

Wakhaloo, S. N. and Shah, S. K., 1970, "Tectonic framework of western Pir Panjal", *Publ. Centr. Ad. Stud. Geol. Panjab University*, **7**, 130-134.

Zahradník, J., Serpetsidaki, A., Sokos, E. and Tselentis, G. A., 2005, "Iterative deconvolution of regional waveforms and a double-event interpretation of the 2003 Lefkada earthquake, Greece", *Bulletin of the Seismological Society of America*, **95**, 1, 159-172.